IEEE Access
Multidisciplinary ⋮ Rapid Review ⋮ Open Access Journal

Received December 7, 2021, accepted December 20, 2021, date of publication December 23, 2021,
date of current version January 5, 2022.

Digital Object Identifier 10.1109/ACCESS.2021.3137908

Investigation of Temperature Sensing Capabilities of GaN/SiC and GaN/Sapphire Surface Acoustic Wave Devices

GEORGE BOLDEIU[1,2], GEORGE E. PONCHAK[3], (Fellow, IEEE), ALEXANDRA NICOLOIU[1], CLAUDIA NASTASE[1], IOANA ZDRU[1], ADRIAN DINESCU[1], AND ALEXANDRU MÜLLER[1], (Member, IEEE)

[1]IMT-Bucharest, 07719 Bucharest, Romania
[2]Faculty of Electronics, Telecommunications and Information Technology, Polytehnica University of Bucharest, 061071 Bucharest, Romania
[3]NASA Glenn Research Center, Cleveland, OH 44135, USA *(Retired)*

Corresponding author: Alexandra Nicoloiu (alexandra.nicoloiu@imt.ro)

This work was supported in part by Grant of the Romanian Ministry of Research, Innovation and Digitalization, CCCDI—UEFISCDI, (dualSAW, 2020–2022), within PNCDI III, under Project PN-III-P2-2.1-PED-2019-0694; and in part by the Romanian of Research, Innovation and Digitalization (Core program) under Contract 14N/2019 MICRO-NANO-SIS PLUS.

ABSTRACT This paper proposes high sensitivity temperature sensors based on single port surface acoustic wave (SAW) devices with GHz resonance frequencies, developed on GaN/SiC and GaN/Sapphire, which permit wide range, accurate temperature determinations. In contrast with GaN/Si SAW based temperature sensors, SiC and Sapphire substrates enable the proper functionality of these devices up to 500°C (773 K), as the high resistivity Si substrate becomes conductive at temperatures exceeding 250°C (523 K) due to the relative low bandgap (and high intrinsic carrier concentrations). Low temperature measurements were carried out using a cryostat between -266°C (7 K) and room temperature (RT) while the high temperature measurements are made on a modified RF probe station. A polynomial fit was used below RT and a linear approximation was evidenced between RT and 500°C (773 K). The structures were simulated at different selected temperatures based on a method that couples Finite Element Method (FEM) and Coupling of Modes (COM). The measured temperature coefficient of frequency (TCF) is about 46 ppm/°C for GaN/SiC SAWs and reaches values of 96 ppm/°C for GaN/Sapphire SAW in the temperature range 25 – 500°C (298 K – 773 K).

INDEX TERMS Surface acoustic wave, temperature sensor, GaN, SiC, sapphire, high temperature measurements, low temperature measurements.

I. INTRODUCTION

Surface acoustic wave (SAW) sensor devices capable of operating at very low temperatures and also at high temperatures bring the possibility of harsh environment applications in industry and in space, due to their full compatibility with wireless data transmission and battery-less operation. Wide bandgap semiconductor piezoelectric materials, grown by MOCVD techniques (such as GaN) or respectively deposited by magnetron sputtering (like AlN) on different substrates, can be used in high sensitivity sensor fabrication due to the potentially higher resonance frequency, with beneficial effects on the sensitivity.

GaN/Si, GaN/SiC and GaN/Sapphire layered structures are fully compatible with nanolithographic and micromachining processes that can be introduced in the fabrication protocol of the acoustic devices (SAW or thin film bulk acoustic resonators). These substrates are intensively used in industrial fabrication of Monolithic Microwave Integrated Circuits (MMICs).

GaN offers the possibility to integrate, on a single chip, SAW sensors with HEMT transistors [1] and also to fabricate multi-detector sensor arrays. An application of temperature SAW sensors might be the temperature monitoring in high power GaN based MMICs for radar applications. As the

The associate editor coordinating the review of this manuscript and approving it for publication was Jiansong Liu.

This work is licensed under a Creative Commons Attribution 4.0 License. For more information, see https://creativecommons.org/licenses/by/4.0/

SAW temperature sensor is compatible with wireless reading and can be monolithic integrated in the circuit, it can be placed very close to the strong heated area of the circuit, the high-power amplifier (HPA) area. In most sensor applications, a high resonance frequency is an advantage since the sensitivity is proportional with the resonance frequency for temperature and pressure sensors [2]. Also, for GaN and AlN based one port SAW temperature sensors, it was evidenced by the authors that "the absolute" value of the sensitivity (the temperature coefficient of frequency- TCF) is higher, if the pitch of the structure is decreased [3].

First results regarding GaN SAW structures (GaN/Sapphire) resonating above 2 GHz have been reported by Palacios in 2002 (2.225 GHz) [4]. An analysis of superior guided SAW propagation modes that appear on GaN/SiC have been reported in [5]. In previous works, the authors reported the first SAW devices on GaN/Si operating at frequencies beyond 5 GHz [6], [7], with Sezawa propagation mode resonance frequencies 15% higher than the fundamental (Rayleigh) mode frequencies [8].

Very recently, AlGaN/GaN/Si heterostructures have been used to fabricate temperature SAW sensor devices (in the range of 77 K to 773 K) for extreme temperature applications. It was demonstrated that the TCF and Q factor of the SAW devices can be engineered by doping of GaN thin film [9].

Most of our previous investigations were focused on SAW sensors manufactured on GaN/Si and AlN/Si thin piezoelectric layers [3], [10]. Very high sensitivities and absolute TCF values (in the range of 62 ppm/°C to 72 ppm/°C) were extracted between 23°C to 150°C for one port SAW resonators on GaN/Si with a resonance frequency between 5.4 and 8.5 GHz [11] and up to 117 ppm/ °C for AlN/Si SAW structures [3]. Although GaN and AlN are wide bandgap semiconductor materials, the silicon substrate seriously limits high temperature performances of sensors manufactured on these materials. If the operating temperature is below 250 - 300°C (523 - 573 K), the silicon substrate is still useful. At higher temperatures, the silicon substrate becomes conductive due to the relative low band gap (and its high intrinsic carrier concentration). If sensors devoted to higher temperature operation are needed, substrates with a higher band gap (and lower intrinsic carrier concentration) are necessary.

SiC is a very good wide bandgap semiconductor material for high temperature and harsh environment operation [12], due to its wide band gap (2.3 to 3.4 eV), high Young modulus (4H-SiC – 460 GPa [13]) and high thermal conductivity (500 W/mK, compared to the thermal conductivity of Si, 150 W/mK). Sapphire has a melting point at 2040 °C, and it has extremely high chemical stability even at high temperatures. Sapphire's energy gap of 9.1 eV is one of the largest for oxide crystals [14]. GaN can be easily grown by MBE and MOCVD techniques on SiC and Sapphire.

Recently, AlN/Sapphire SAW devices have attracted attention for high frequency applications and proved their reliability for high temperature [15], [16], while GaN/Sapphire substrate was more investigated for SAW UV sensing [17], [18] and less for temperature sensors [19].

Fig. 1 presents a comparison of the TCF of several temperature sensors from literature on different substrates, including the present work. T. Aubert *et al.* have been focused in the last years on high temperature SAW sensors based on AlN/Sapphire bilayer structures and proved good TCF = −80 ppm/°C [15] and very high Q factors – 8000 at room temperature [16]. They also proposed an improved AlN/IDT/GaN/Sapphire SAW structure (TCF = −34.6 ppm/°C) starting from a SAW device on GaN/Sapphire with Al metallization of the IDTs (TCF = −29.6 ppm/°C) in order to develop a packageless temperature SAW sensor able to operate up to 500°C [19]. A gigahertz operating SAW temperature sensor based on AlN/Sapphire with a TCF of −38.6 ppm/°C was presented in [20].

A SAW sensor with a resonance frequency of 549 MHz, fabricated on Mo/AlN/6H-SiC, has shown a high TCF value of 90 ppm/°C in the 25°C – 300°C temperature range [21].

This article proposes two SAW temperature sensors developed on GaN/4H-SiC and on GaN/Sapphire using advanced nanolithographic tools. The sensors are devoted for a very large temperature range, between −266°C (∼7K) and 500°C (773K), exhibiting superior performances: higher resonance frequencies (4.26 GHz – GaN/SiC SAW; 2.98 GHz – GaN/Sapphire SAW) and higher absolute value of the TCF calculated between RT and 500°C (96.5 ppm/°C - GaN/Sapphire SAW). In this paper we demonstrate the importance of coupling FEM and COM simulation methods for more accurate results of the envisaged sensors.

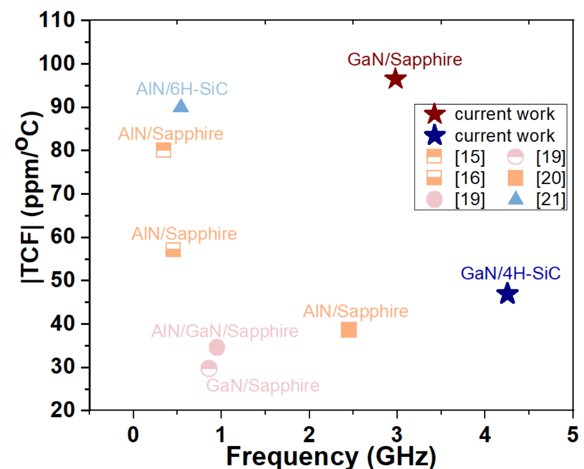

FIGURE 1. Different sensors performance comparison in terms of TCF and resonance frequency, including the work presented in this paper.

II. SIMULATION PROCEDURE

In literature, several techniques were developed for the simulation of the SAW devices, based on COM theory, P-matrix or equivalent circuits [22], [23]. The accuracy of the COM model is based on taking into account several parameters, such as: the SAW velocity, reflectivity, attenuation,

frequency, and transduction. All these parameters can be determined experimentally or by FEM. In order to enhance the electric response of the SAW devices, a coupled FEM - COM theory was recently developed by our group for AlN/Si SAW temperature sensors [3] and addressed in the current paper in a systematic manner for the GaN/SiC and GaN/Sapphire SAW devices.

A. THEORETICAL BACKGROUND AND COM MODEL

SAW devices are based on the piezoelectric effect which couples the interaction between electromagnetic and acoustic waves. The constitutive equations for piezoelectric effect are given by:

$$T_{ij} = C^E_{ijkl} S_{kl} - e_{kij} E_k \tag{1}$$

$$D_i = e_{jkl} S_{kl} - \varepsilon^S_{ij} E_i \tag{2}$$

where $\boldsymbol{T}$ represents the stress tensor, $\boldsymbol{S}$ the strain tensor, $\boldsymbol{D}$ the electrical displacement vector, $\boldsymbol{E}$ the electric field vector, $\boldsymbol{C}$ the elastic tensor, $\boldsymbol{\epsilon}$ the electrical permittivity tensor and, e the piezoelectric tensor.

Substituting in equation (1) the strain $S_{kl} = \frac{1}{2}\left(\frac{\partial u_l}{\partial x_k} + \frac{\partial u_k}{\partial x_l}\right)$, where u_k and u_l represent the displacement and $E_k = -\nabla\Phi$, (1) becomes:

$$\rho \frac{\partial^2 \mathrm{x_i}}{\partial \mathrm{t}^2} = \mathrm{C^E_{ijkl}} \frac{\partial \mathrm{u_l}}{\partial \mathrm{x_k}} + \mathrm{e_{kij}} \frac{\partial \Phi^2}{\partial \mathrm{x_j x_k}} \tag{3}$$

The solid must satisfy the Poisson's equation $\partial D_j / \partial x_j = 0$ and equation (2) becomes:

$$\mathrm{e_{jkl}} \frac{\partial^2 \mathrm{u_l}}{\partial \mathrm{x_j} \partial \mathrm{x_k}} - \epsilon_{jk} \frac{\partial^2 \Phi}{\partial \mathrm{x_j} \partial \mathrm{x_k}} = 0 \tag{4}$$

where ρ is the mass density of the material, and Φ is the electrical potential. The influence of the temperature on SAW adds a new strain and the thermal expansion strain equation is:

$$S_{th} = \alpha\left(\Theta - \Theta_{ref}\right) \tag{5}$$

where α is the coefficient of thermal expansion, S_{th} is the thermal strain, and Θ is the temperature.

The COM theory describes the interaction between two waves that propagate in opposite directions. The governing equations are:

$$\begin{aligned} \frac{dR}{dx} &= -i\delta R - ik^* Q + i\alpha V e^{-i\beta x} \\ \frac{dQ}{dx} &= i\delta Q + ikR - i\alpha^* V e^{-i\beta x} \\ \frac{dI}{dx} &= -2i\alpha^* - 2i\alpha Q + i2\pi f C V e^{-i\beta x} \end{aligned} \tag{6}$$

where R and Q are the amplitudes of waves, δ (the most important parameter of COM model) is the detuning parameter ($\delta = 2\pi\,(f - f_0)\,/\,(v - i\gamma)$), I is the electrical current of the IDT, V is the applied voltage, C is the electrical capacitance and $\omega = 2\pi$ is the angular frequency. In equation (6), the symbol $*$ represents the complex conjugate parameter [22]. The rest of parameters are given in Table 1.

TABLE 1. COM parameters.

Parameter	Symbol
SAW velocity	v_{SAW}
Reflectivity	$k_p = \lambda_0 k$
Transduction coefficient	$\alpha_p = \lambda_0\,\alpha$
Normalized transduction	$\alpha_n = \alpha_0\sqrt{W/\lambda_0}$
Attenuation	$\gamma_p = \lambda_0$
Capacitance	$C_p = \lambda_0 C$
Normalized capacitance	$C_n = C_p/W$

B. SIMULATION STEPS

The initial simulations are performed in COMSOL Multiphysics (the FEM based software used for the current work); the output results are used as input in COM. The first step in the simulation process is the short circuit simulation (top of piezoelectric layer is covered with a metallization layer) which provides the values for the velocity and reflectivity of the SAW. The second simulation, open circuit, determines the electrical capacitance and the third is carried out in frequency domain (harmonic regime) in order to find the values of transduction and attenuation coefficients. All these parameters are introduced into a script file with the COM model to calculate the values of admittance as a function of frequency.

1) SIMULATION OF THE SHORT CIRCUIT

The short circuit configuration is used to extract the value of the velocity and reflectivity (i.e., $\boldsymbol{V} = \boldsymbol{0}$ and $\boldsymbol{\gamma} = \boldsymbol{0}$, no attenuation) [22], [24].

$$v_{SAW} = \frac{\lambda}{2}\left(f^+_{SC} + f^-_{SC}\right) \tag{7}$$

$$k = \frac{\pi}{v_{SAW}}\left(f^+_{SC} - f^-_{SC}\right) \tag{8}$$

where $f^{+,-}_{SC}$ are the stopband edges of the short circuit dispersion relation.

2) SIMULATION OF THE OPEN CIRCUIT

Usually, the open circuit simulation is performed simultaneously with the harmonic admittance simulation in order to calculate the electrical capacitance and the attenuation. For our model, this approach was replaced by a simple electrostatic simulation in FEM in order to calculate the electrical capacitance of one pair of IDT fingers [22].

3) SIMULATION OF THE HARMONIC ADMITTANCE

The outcome of the frequency domain simulation is the admittance curve, from which the following parameters are extracted: Δf - half width frequency difference, Y_{max} - the maximum value of admittance, α_p - the transduction coefficient and the attenuation coefficient - $\gamma = 0$ [22]:

$$Y_{max} = \frac{4\alpha_p^2}{\gamma_p} \tag{9}$$

$$\Delta f = \frac{f_0 \gamma_p}{\pi} \quad (10)$$

4) P-MATRIX AND RESISTIVITY OF THE FINGER

In order to extract an admittance for the SAW devices with an increased accuracy, P-matrix is used together with the COM parameters, determined in the previous steps. The P-matrix is:

$$\begin{bmatrix} P_{11}(f) & P_{12}(f) & P_{13}(f) \\ P_{21}(f) & P_{22}(f) & P_{23}(f) \\ P_{31}(f) & P_{32}(f) & P_{33}(f) \end{bmatrix}, \quad (11)$$

where $\boldsymbol{P_{11}}$ and $\boldsymbol{P_{22}}$ are the reflection coefficients, $\boldsymbol{P_{12}} = \boldsymbol{P_{21}}$ is the transmission coefficient, $\boldsymbol{P_{13}}$ and $\boldsymbol{P_{23}}$ describe the excitation efficiency of the IDT and $\boldsymbol{P_{31}}$ and $\boldsymbol{P_{32}}$ measure the current generated by the waves in the IDT and the final $\boldsymbol{P_{33}}$ describes the acoustic and electrostatic currents due to the driven voltage.

The admittance describes the acoustic and electrostatic current due to the driving voltage V and is given by the formula [22]:

$$Y = P_{33} - \frac{4RP_{13}^2}{1 - R\left(P_{11} + P_{12}\right)} \quad (12)$$

where R denotes the reflection coefficient of reflectors. Also, the value of the finger resistivity was taken into account and the formula for single electrode transducer is [22]:

$$R_{finger} = \frac{2W}{3a}\rho_{\blacksquare} \quad (13)$$

where W is the aperture, a is the width of electrode and $\boldsymbol{\rho_{\blacksquare}}$ is the square resistivity of the metal [22].

III. SIMULATION RESULTS

Due to the high ratio between the thickness and the length of the IDT structure, the simulation of the whole three-dimension (3D) model would be time consuming, so a 2D model was implemented. Moreover, COMSOL Multiphysics takes into consideration the periodicity of the structure, allowing us to reduce the model even more, to one period, $\lambda = 4 \cdot w$, where w represents the width of the finger and the interdigit spacing of the IDT. The model geometry (Fig. 2) consists of one pair of fingers (the wavelength, λ is 1.6 μm for the SAW on GaN/SiC and 2 μm for the SAW on GaN/Sapphire). The thickness of the IDTs metallization, h_{Au}, is 80 nm. The GaN layer (1.2 μm thin) is placed on top of the substrate (SiC or Sapphire) domain, reduced to 50 μm thick. A perfectly matched layer (PML) of 10$\boldsymbol{\lambda}$ was introduced below, with the role to retain the wave reflections from the bottom [25]. The Boundary conditions imposed for the mechanical and electrical simulations are presented in Table 2.

Usually, the temperature affects the properties of the materials. If a linear model is used to calculate the mechanical, electrical and thermal properties for SiC, Sapphire and Au, their variation is almost negligible. It is difficult to use a certain type of model for the substrate and another one for the metallization. For these structures, it was assumed that these material properties are constant with the change of temperature as depicted in Table 3. On the other hand, GaN piezoelectric properties were modified by a nonlinear model extracted from [26].

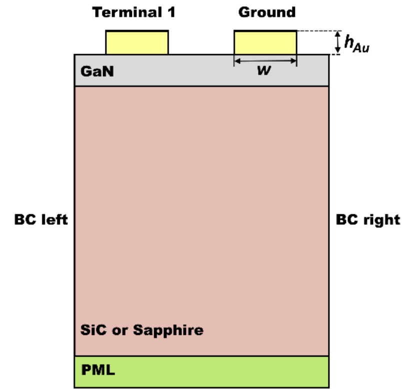

FIGURE 2. The 2D model simulated in Comsol Multiphysics.

TABLE 2. Boundary conditions for mechanical and electrical simulations.

Boundary	Short circuit	Harmonic admittance	Open grating	Mechanical
BC left BC right			$\Phi_{BCl} = \Phi_{BCr}$	$u_{iBCleft} = u_{iBCright}$
Terminal 1	$\Phi = 0$	$\Phi = \cos(\omega \cdot t)$	$\int D \cdot n = 0$	$\sigma_{ij} n = 0$
Ground	$\Phi = 0$	$\Phi = 0$	$\int D \cdot n = 0$	$\sigma_{ij} n = 0$
Bottom			$\Phi = 0$	$u_i = 0$

TABLE 3. Material properties of The Substrate (SiC, Sapphire) and of the Electrode Metallization (Au).

Material property	Units	SiC	Sapphire	Au
Density, ρ	kg/m^3	3211	3980	19000
Young modulus, E	GPa	460.73	400	70
Poisson ratio, ν	-	0.18	0.29	0.44
CTE, α	1/K	4.3x10^{-6}	4.5x10^{-6}	14.2x10^{-6}
Relative permittivity, ε	-	9.66	11.6	

The elastic coefficients for GaN at different temperatures are presented in Table 4.

The FEM simulation first extracts the eigenfrequencies (f_{sc}^- and f_{sc}^+) and the capacitance, succeeded by the extraction of the admittance from the harmonic simulation, as explained in Chapter II.B. A flowchart with the implemented simulation technique was first presented for AlN/Si SAW temperature sensors up to 150°C in [3]. A comparison between the real part of the admittance extracted from FEM simulations, the coupled FEM and COM technique and the measurements is presented in Fig. 3a for the GaN/SiC

TABLE 4. Elastic properties of GaN at different temperatures [26].

T	C_{11}	C_{33}	C_{12}	C_{13}	C_{44}	E
[K]	[GPa]	[GPa]	[GPa]	[GPa]	[GPa]	[GPa]
0	376.4	387.1	142.4	99.1	98.5	289.5
50	376.4	387.1	142.4	99.1	98.5	289.5
100	376.1	386.8	142.3	99.0	98.5	289.3
200	375.4	385.8	141.9	98.7	98.4	288.9
300	374.2	384.4	141.4	98.1	98.3	288.1
400	372.6	382.3	140.6	97.4	98.1	287.2
500	370.7	380.0	139.8	96.7	97.9	286.0

SAW structure and in Fig. 3b for GaN/Sapphire SAW device. The Y experimental curves are extracted from the S-measurements of the fabricated devices (presented in the following chapter). The FEM simulation gives a good response in terms of the resonance frequency, particularly at room temperature – the error between measurements and FEM is 0.9% for the GaN/SiC structure and 2.2% for GaN/Sapphire SAW device. These differences are significantly reduced when COM method is included in the simulation procedure – the error becomes 0.07% for the GaN/SiC structure and 0.31% for GaN/Sapphire. These errors increase with the temperature change and COM simulation becomes essential as it takes into account the behavior of the whole structure, including the number of IDT pairs and the reflectivity.

The graphs from Fig. 3 present the admittances extracted from the coupled FEM and COM simulation, evidencing a better agreement to measurements, than the FEM simulation. It can be noticed that the maximum amplitude (Y_{max}) of the real part of the admittance extracted from the coupled COM and FEM technique is two orders of magnitude higher than the values extracted directly from FEM simulations and the response is closer to measurements.

The values of the u and v displacement in x and y directions are extracted at room temperature along the top boundary of the GaN layer (Fig. 4). The two displacements have the same characteristic at resonance frequency (4.21 GHz – GaN/SiC SAW device and 3.05 GHz – GaN/Sapphire SAW device) and the maximum values are reached on the y direction, on the electrodes – 0.8 nm for the GaN/SiC SAW and 4 nm for the GaN/Sapphire SAW.

IV. EXPERIMENTAL RESULTS AND DISCUSSION

A. FABRICATION PROCESS

The GHz operating single SAW resonators were fabricated on GaN/SiC and GaN/Sapphire wafers commercially obtained from NTT-AT, Japan. The GaN layer was grown by Metal-Organic Chemical Vapor Deposition (MOCVD), on 4H - SiC substrate (0.7 μm thickness, including the buffer of 0.2 μm) with high resistivity (>105 Ω·cm) and (0001) crystallographic orientation and respectively on Sapphire substrate (1 μm thickness).

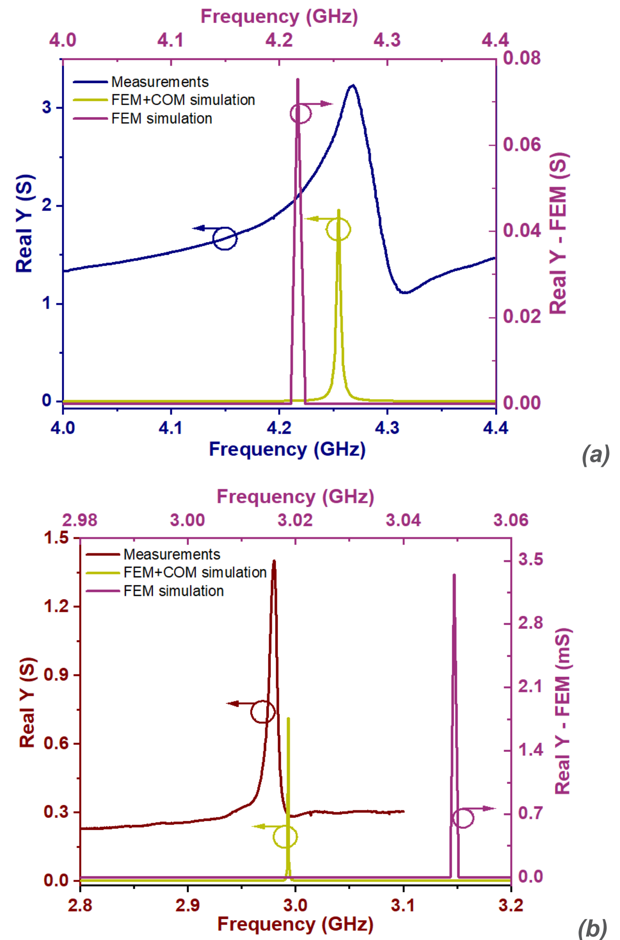

FIGURE 3. The real part of the admittance at 25°C extracted from the coupled FEM – COM simulation (yellow) compared to the measurements and to FEM simulation (magenta) for: (a) GaN/SiC SAW structure and (b) GaN/Sapphire SAW structure.

The fabrication process is similar to the development of the SAW devices on GaN/Si wafers, presented by the authors in the past [6], [10]. The IDTs and the reflectors were defined by electron beam lithography and the lift-off technique. For RF characterization, coplanar waveguide pads Ti/Au 40 nm/400 nm were employed by photolithography and lift-off processes. The design parameters of the SAW devices are summarized in Table 5.

TABLE 5. SAW devices properties.

	GaN/SiC	GaN/Sapphire
IDT finger width, w [nm]	400	500
IDT finger length, [µm]	50	50
Ti/Au thickness on IDTs, h_{Au} [nm]	5/75	5/75
No. of IDT fingers	150	150
No. of reflectors	50	50

A 3D schematic of the SAW structures, including the measuring pads is shown in Fig. 5a. Fig. 5b presents SEM photos

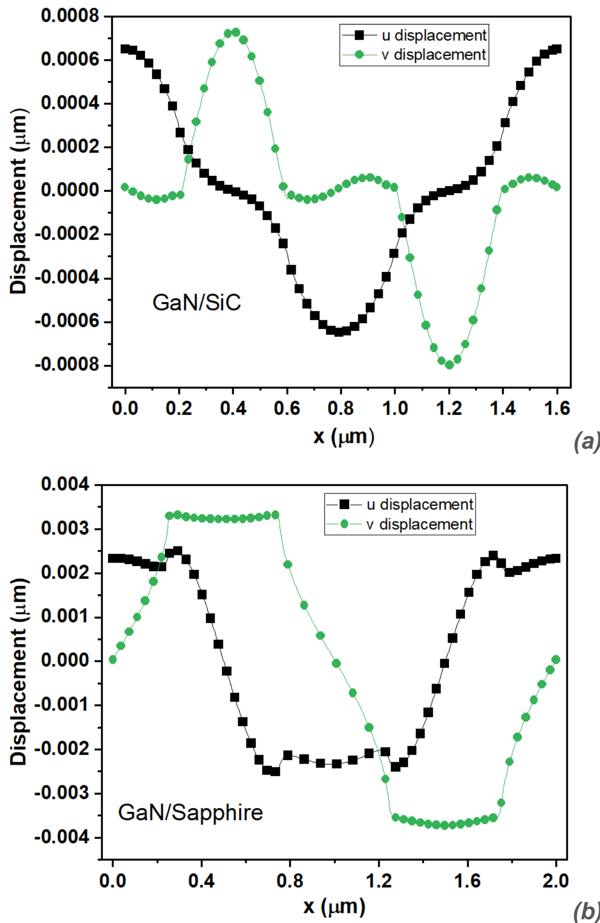

FIGURE 4. The displacement in x (black) and y (green) direction at resonance frequency at RT for: (a) GaN/SiC SAW and (b) GaN/Sapphire SAW structure.

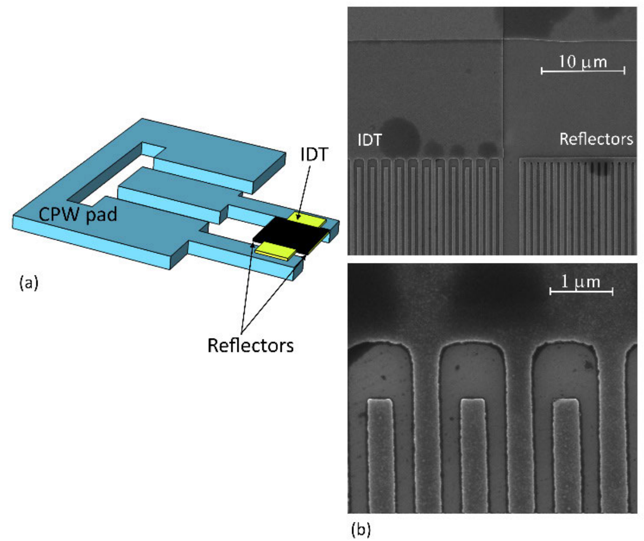

FIGURE 5. (a) 3D schematic of the SAW structures; (b) SEM photos of the IDTs for the SAW device on GaN/SiC with w = 400 nm.

of the IDTs, evidencing the nanolithography for fingers and interdigit spacing 400 nm wide developed on GaN/SiC. In order to measure the temperature sensing structures in a wider temperature range, the wafers were diced into chips. The temperature dependence of the resonance frequency for the manufactured SAW structures was determined using the electrical reflection parameter (S_{11}).

B. LOW TEMPERATURE MEASUREMENT PROCEDURE

The low temperature measurements were carried out using a cryostat (SHI-4H-1 from Janis Research Company) able to perform measurements in the 5–500 K temperature range. This cryostat operates with recirculating He (i.e. without He consumption) and is able to cool down to 5 K, being intended by the manufacturer only for low temperature DC measurements. In order to allow on-wafer measurements in the microwave and mm-wave frequency ranges, a special test fixture was designed and manufactured in-house (Fig. 6). The test fixture was built with Picoprobe 67A-GSG-100-P (GGB Industries Inc.) on-wafer test probes with 7.85 mm female connector and low-loss coaxial cables, capable to operate up to 67 GHz and to test structures with 150 μm pitch padframe, in ground-signal-ground (GSG) configuration. The major challenge was to build the x, y, z movable plate where the chip is placed and where the millimetre wave probes touch down to contact the device under test (DUT). The entire test fixture had to fit the standard dimensions of the cryostat.

The SAW devices were assembled on a metallic fixture inserted in the cryostat, which was connected to a Vector Network Analyzer (VNA - MS46122A Anritsu) through probe tips (150 μm pitch), allowing S-parameter measurements. Fig. 7a and 8a show the frequency response of the two SAW structures at different temperatures between RT and −266°C (7 K). The resonance frequency variation in this temperature range has a parabolic nature, evidenced by a polynomial fit of 2nd degree (Fig. 7b for the structure on GaN/SiC and Fig. 8b for GaN/Sapphire SAW). Between −93°C (180 K) and 25°C (298 K) a linear fit was applied in order to determine the TCF. The measured TCF is −30 ppm/°C for GaN/SiC SAW device and −49 ppm/°C for the GaN/Sapphire SAW. At cryogenic temperatures, below −200 °C (73 K) the resonance frequency of both SAW structures has a lower temperature variation and the TCF starts to decrease. This temperature range is appropriate for acoustic devices manufactured on GaN used in applications where temperature stability is required.

The coupled FEM+COM simulation procedure was selectively applied in order to determine the resonance frequency variation with respect to temperature between 25°C (298 K) and −266°C (7 K) (inset of Fig. 7b for GaN/SiC SAW and inset of Fig. 8b for GaN/Sapphire SAW). The simulated variation shows a linear behavior, unlike the measurements because the initial FEM simulation does not include the change of the thermal expansion coefficient with temperature. Even the behavior is not the same, the difference between the resonance frequencies extracted from measurements and simulations is insignificant (errors are less than 0.3% for both structures).

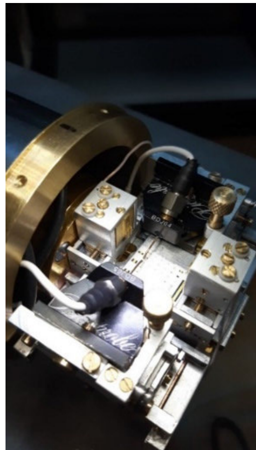

FIGURE 6. The in-house setup built for microwave measurements inside the cryostat.

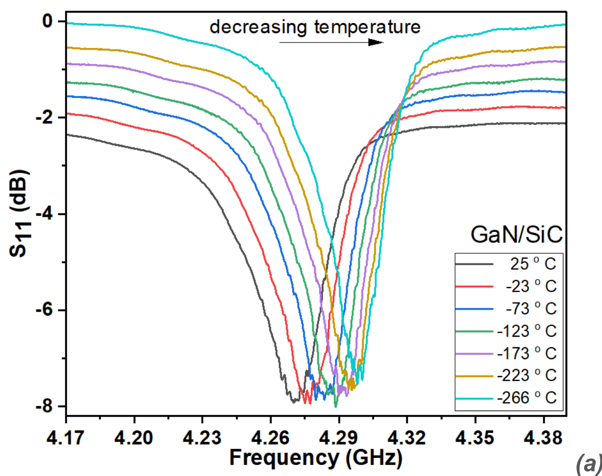

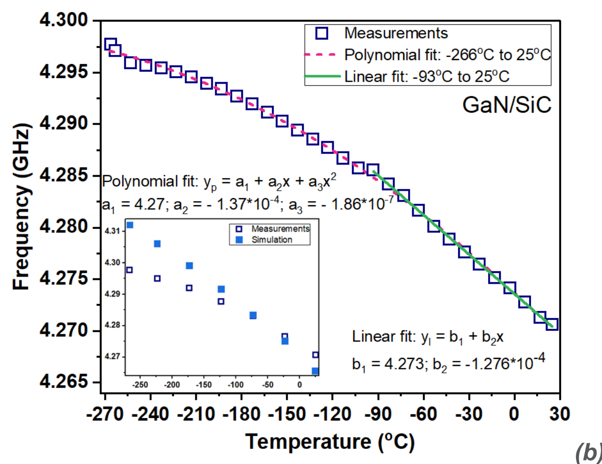

FIGURE 7. (a) Measured S_{11} parameter vs. temperature and (b) the linear fitting for the experimental resonance frequency variation vs. temperature between −266°C and 25°C; inset: comparison between the simulated (FEM+COM) and measured resonance frequencies for the SAW structure on GaN/SiC.

C. HIGH TEMPERATURE MEASUREMENT PROCEDURE

The SAW resonators were characterized on a modified RF probe station comprised of a wafer chuck built from a thermal

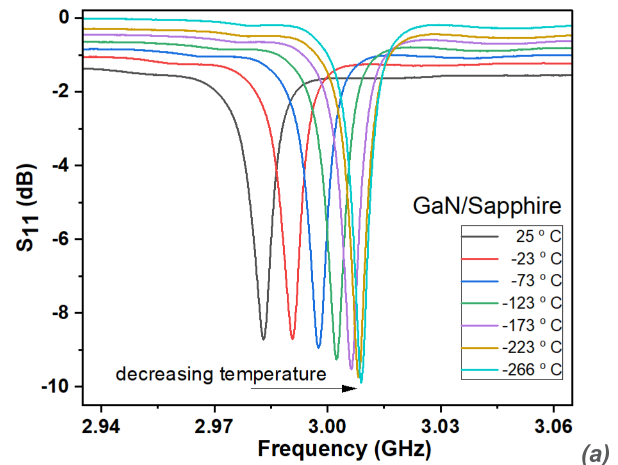

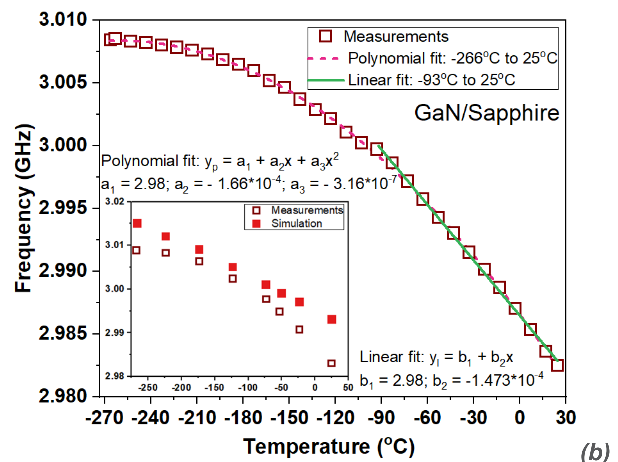

FIGURE 8. (a) Measured S_{11} parameter vs. temperature and (b) the fitting for the experimental resonance frequency variation vs. temperature between −266°C and 25°C; inset: comparison between the simulated (FEM+COM) and measured resonance frequencies for the SAW structure on GaN/Sapphire.

insulator, a ceramic heater, a thermo couple held in intimate contact with the ceramic heater, a LabView program to control the heater temperature, and a 150 μm pitch, GSG, modified GGB Picoprobe [27]. The temperature of the SAW device and the thermocouple placed on an Alumina wafer are assumed to be equal. Because the RF probe is held in place on the SAW device during the heating and stabilization time of the heater, the RF probe tip is at the same temperature as the SAW device [27]. An Agilent PNA was used for the measurements, with 16,000 data points and a frequency span set to achieve data points separated by approximately 9.4 kHz. An Open-Short-Load calibration was performed at RT, over the frequency range of the measurements, using a GGB Picoprobe calibration standard that placed the reference plane at the probe tips. A photograph of the SAW resonator being characterized is shown in Fig. 9a.

The temperature was increased in 10°C increments, and it took approximately 3 minutes to increase the temperature to the new set point. The measurements were taken once the temperature stabilized, which typically took 60 seconds.

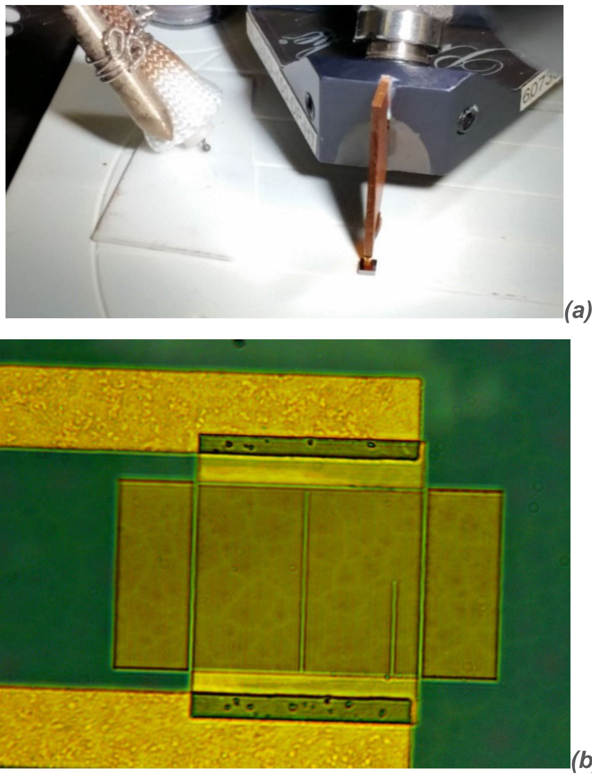

FIGURE 9. **(a) Photograph of Surface Acoustic Wave Resonator under test on modified probe station; (b) Surface Acoustic Wave resonator with Ti/Au metallization after testing at 500°C.**

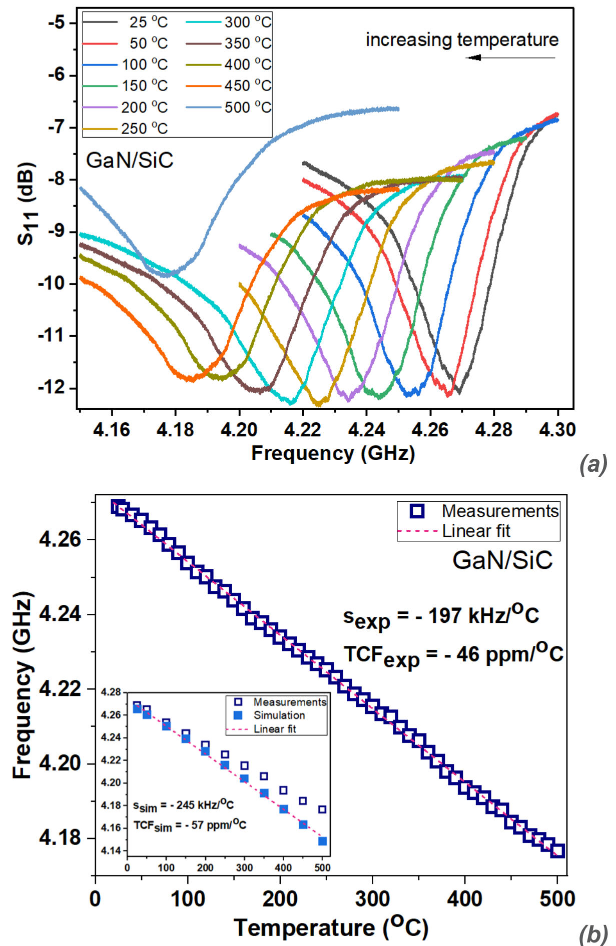

FIGURE 10. **(a) Measured S_{11} parameter vs. temperature and (b) the linear fitting for the experimental resonance frequency variation vs. temperature between 25°C and 500°C; inset: comparison between the simulated (FEM+COM) and measured resonance frequencies for the SAW structure on GaN/SiC.**

Each SAW resonator was measured three times. The first two measurements overlap, while the third one showed a difference below 300°C (573 K). The standard deviation for all three measurements is around $5 \cdot 10^{-3}$ below 300°C (573 K) and $0.8 \cdot 10^{-3}$ above 300°C (573 K). The measurements were made on consecutive days and the sample was cooled to room temperature and the system was recalibrated before each measurement.

Devices with Ti/Au metallization operated through 500°C, with the only visual effects being diffusion of Ti through the Au, as shown in Fig. 9b. Ti/Au metallization has been shown to be a stable metallization previously [28].

Fig. 10a shows selected reflection parameters, S_{11}, for the GaN/SiC SAW device between RT and 500°C (773 K). It is evident that the resonance frequency of the structure shifts to lower values as the temperature increases due to the expansion of the piezoelectric layer (GaN). A similar behavior is observed for the GaN/Sapphire SAW structure as depicted in Fig. 11a.

A linear behavior in the resonance frequency change is observed between RT and 500°C (773 K) for both measured devices. The simulated resonance frequency (extracted from the coupled FEM+COM technique) at different temperatures is compared to the experimental results in the insets of Fig. 10b for the GaN/SiC SAW structure and in the inset of Fig. 11b for the GaN/Sapphire SAW device. A very good agreement between the resonance frequencies was observed between the experimental and simulated values when temperature is varied between 25°C and 500°C. The difference increases with the temperature change, especially above 150°C. For the GaN/SiC structure (Fig. 10b) the error between the simulation and experiment is quite constant with the temperature change - varies between 0.07% at RT to 0.65% at 500°C (773 K). For the GaN/Sapphire SAW device (Fig. 11b) the error between simulation and measurement reaches 3.5% at 500°C (773 K).

The sensitivity s = df/dT (expressed in kHz/°C), and the TCF (expressed in ppm/°C) were extracted from the slope of the resonance frequency as function of temperature (Fig. 10b and Fig. 11b) from both simulation and experiment. It is interesting to notice that the GaN/Sapphire SAW device has a higher absolute value of the TCF (96.5 ppm/°C) than the GaN/SiC structure (46 ppm/°C), even if the resonance frequency is lower. Also, the sensitivity and the TCF obtained from simulation differs from the experiment and this is explained by the incomplete information regarding the variation of the material parameters with the temperature. The

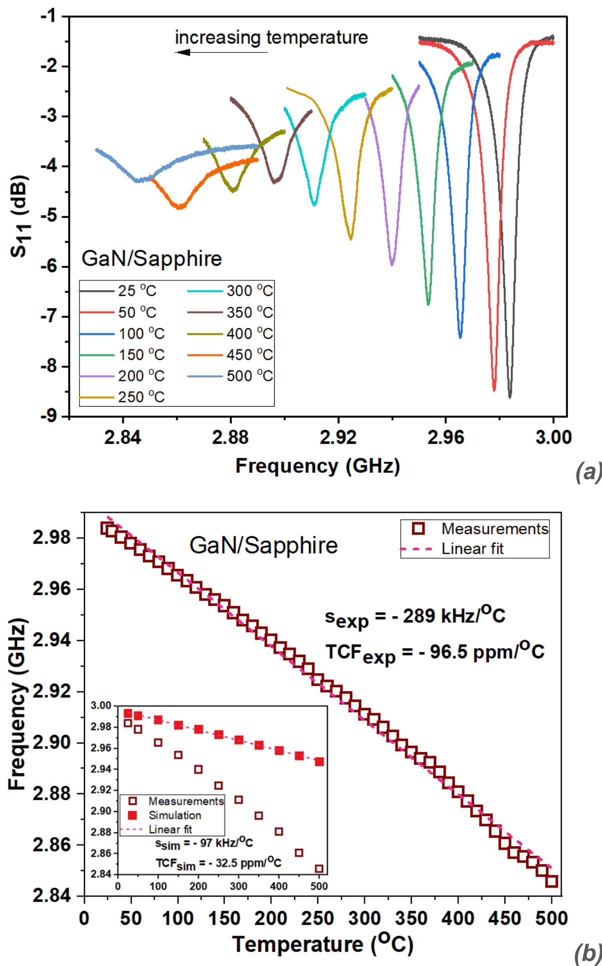

FIGURE 11. **(a) Measured S_{11} parameter vs. temperature and (b) the linear fitting for the experimental resonance frequency variation vs. temperature between 25°C and 500°C; inset: comparison between the simulated (FEM+COM) and measured resonance frequencies for the SAW structure on GaN/Sapphire.**

values of the sensitivity and TCF are comparable to those obtained by the authors for similar SAW structures on GaN/Si measured up to 150°C [10], [11].

A study of the evaluation of the quality factor (Q) and the effective coupling coefficient (k^2_{eff}) as function of the temperature has been performed in the −266°C (7K) to 500°C (773 K) temperature range. Both, Q and k^2_{eff} could be extracted from the S parameter measurements performed on this temperature range. At room temperature the obtained values of the Q and k^2_{eff} of GaN/SiC were 182 and respectively 2.8%; for GaN/Sapphire the Q was 757 and k^2_{eff} was 0.62%. The k^2_{eff} increases with temperature while Q shows a quasi-linear decreasing trend versus temperature, similar to what was reported in literature for AlN/Sapphire [16], [20].

Although the results are promising and the device visual aspect remained unchanged after a number of cycles from very low temperatures to 500°C (773 K) (Fig. 9b), the use of Au based metallization system does not represent a reliable solution for temperatures beyond 250°C (523 K). The titanium barrier between the gold and the semiconductor has a positive influence and devices could be tested properly, but long-term operation needs some radical changes in the metallization system. A reliable behavior of the sensor, in the entire temperature analyzed range needs the development of another metallization system both for the IDTs as well as for the connection pads. A relative thick (200 – 300 nm) Pt or Ir metallization [29] would be optimal for high temperature operation. On the other hand, a thick metallization of a heavy metal like Pt on the IDTs strongly affects the SAW behavior. For our future work we propose the development of a thick Pt metallization for the connection pads and 40-50 nm thin Mo metallization for the IDTs, as Mo has a very high acoustic impedance, low density [30], [31] and also good high temperature properties.

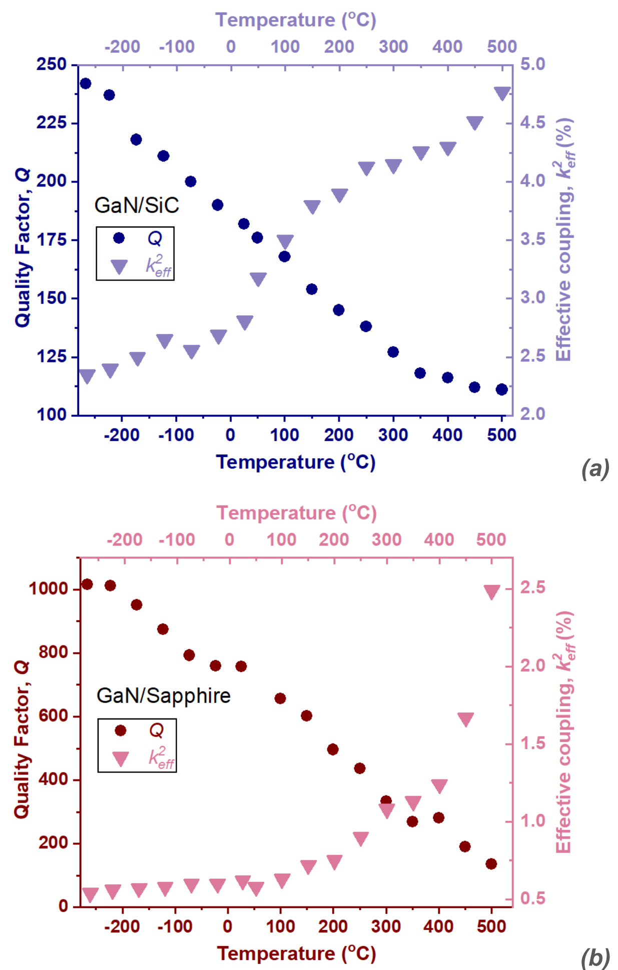

FIGURE 12. **The evolution of the measured quality factor, Q and effective coupling coefficient, k^2_{eff} as a function of temperature for the SAW structure on GaN/SiC (a) and on GaN/Sapphire (b).**

V. CONCLUSION

This paper presented GaN/SiC and GaN/Sapphire SAW structures suitable for wide range temperature sensing – from low temperatures (down to −266°C (7 K)) to very high

temperatures (up to 500°C (773 K)). The simulation method based on FEM and COM techniques was described in detail and the simulated results, at room temperature, were compared to measurements and to FEM simulations in order to evidence the importance of the coupled technique. Furthermore, the fabricated devices were measured in a cryostat down to 7 K and also on a modified RF probe station up to 773 K. The resonance frequency variation between RT and −266°C (7 K) has a parabolic nature, evidenced by a polynomial fit of 2nd degree while between −93°C (180 K) and 25°C (298 K) a linear fit was performed in order to determine the TCF. At cryogenic temperatures, below −200 °C (73 K) the TCF starts to decrease, an important feature for applications where the temperature stability is required.

A linear behavior is observed between 25°C (298 K) and 500°C (773 K) for the measured devices and the simulations with temperature were in very good agreement with the experimental results. The work demonstrates the important contribution of the substrate in high temperature sensing applications. The use of SiC and Sapphire as substrate for the GaN piezoelectric sensing layer make possible temperature determinations up to 500°C (773 K) (our upper temperature limit for the determinations), in contrast with temperature sensors manufactured on GaN/Si which worked properly only for temperatures below 250 – 300°C (523 - 573 K).

ACKNOWLEDGMENT

The authors would like to thank to Mircea Pasteanu for the help in the experimental setup at low temperatures and to Gabriel Craciun for performing the SEM analysis of the SAW structures.

REFERENCES

[1] S. Ghosh, T. Hancock, M. Storey, L. Parameswaran, M. Geis, R. Ralston, and D. Weinstein, ''Nonreciprocal acoustoelectric interaction of surface waves and fluorine plasma-treated AlGaN/GaN 2 DEG,'' in *Proc. 19th Int. Conf. Solid-State Sens., Actuators Microsyst. (TRANSDUCERS)*, Kaohsiung, Taiwan, Jun. 2017, pp. 1939–1942.

[2] J. G. Rodríguez-Madrid, G. F. Iriarte, O. A. Williams, and F. Calle, ''High precision pressure sensors based on SAW devices in the GHz range,'' *Sens. Actuators A, Phys.*, vol. 189, pp. 364–369, Jan. 2013.

[3] A. Nicoloiu, G. E. Stan, C. Nastase, G. Boldeiu, C. Besleaga, A. Dinescu, and A. Müller, ''The behavior of gold metallized AlN/Si- and AlN/glass-based SAW structures as temperature sensors,'' *IEEE Trans. Ultrason., Ferroelectr., Freq. Control*, vol. 68, no. 5, pp. 1938–1948, May 2021.

[4] T. Palacios, F. Calle, J. Grajal, E. Monroy, M. Eickhoff, O. Ambacher, and F. Omnes, ''High frequency SAW devices on AlGaN: Fabrication, characterization and integration with optoelectronics,'' in *Proc. IEEE Ultrason. Symp.*, vol. 1, Oct. 2002, pp. 57–60.

[5] Y. Takagaki, P. V. Santos, E. Wiebicke, O. Brandt, H.-P. Schönherr, and K. H. Ploog, ''Guided propagation of surface acoustic waves in AlN and GaN films grown on 4*H*–SiC(0001)substrates,'' *Phys. Rev. B, Condens. Matter*, vol. 66, no. 15, pp. 1–7, Oct. 2002.

[6] A. Müller, D. Neculoiu, G. Konstantinidis, G. Deligeorgis, A. Dinescu, A. Stavrinidis, A. Cismaru, M. Dragoman, and A. Stefanescu, ''SAW devices manufactured on GaN/Si for frequencies beyond 5 GHz,'' *IEEE Electron Device Lett.*, vol. 31, no. 12, pp. 1398–1400, Aug. 2010.

[7] A. Stefanescu, A. Müller, I. Giangu, A. Dinescu, and G. Konstantinidis, ''Influence of Au-based metallization on the phase velocity of GaN on Si surface acoustic wave resonators,'' *IEEE Electron Device Lett.*, vol. 37, no. 3, pp. 321–324, Mar. 2016.

[8] A. Müller, I. Giangu, A. Stavrinidis, A. Stefanescu, G. Stavrinidis, A. Dinescu, and G. Konstantinidis, ''Sezawa propagation mode in GaN on Si surface acoustic wave type temperature sensor structures operating at GHz frequencies,'' *IEEE Electron Device Lett.*, vol. 36, no. 12, pp. 1299–1302, Dec. 2015.

[9] A. Qamar, S. R. Eisner, D. G. Senesky, and M. Rais-Zadeh, ''Ultra-high-*Q* gallium nitride SAW resonators for applications with extreme temperature swings,'' *J. Microelectromech. Syst.*, vol. 29, no. 5, pp. 900–905, Oct. 2020.

[10] A. Müller, G. Konstantinidis, V. Buiculescu, A. Dinescu, A. Stavrinidis, A. Stefanescu, G. Stavrinidis, I. Giangu, A. Cismaru, and A. Moldoveanu, ''GaN/Si based single SAW resonator temperature sensor operating in the GHz frequency range,'' *Sens. Actuators A, Phys.*, vol. 209, pp. 115–123, Mar. 2014.

[11] A. Müller, G. Konstantinidis, I. Giangu, V. Buiculescu, A. Dinescu, A. Stefanescu, A. Stavrinidis, G. Stavrinidis, and A. Ziaei, ''GaN-based SAW structures resonating within the 5.4–8.5 GHz frequency range, for high sensitivity temperature sensors,'' in *IEEE MTT-S Int. Microw. Symp. Dig.*, Tampa, FL, USA, Jun. 2014, pp. 1–4, doi: 10.1109/MWSYM.2014.6848483.

[12] H.-P. Phan, D. V. Dao, K. Nakamura, S. Dimitrijev, and N.-T. Nguyen, ''The piezoresistive effect of SiC for MEMS sensors at high temperatures: A review,'' *J. Microelectromech. Syst.*, vol. 24, no. 6, pp. 1663–1677, Dec. 2015.

[13] *SiC-Silicon Carbide Properties*. Accesed: Oct. 2021. [Online]. Available: http://www.ioffe.ru/SVA/NSM/Semicond/SiC/

[14] *Sapphire: Physical & Mechanical Properties*. Accesed: Oct. 2021. [Online]. Available: http://www-eng.lbl.gov/~shuman/next/materials%26components/Quartz/Sapphire_Physical_Mechanical_Properties.pdf

[15] T. Aubert, O. Elmazria, B. Assouar, E. Blampain, A. Hamdan, D. Geneve, and S. Weber, ''Investigations on AlN/sapphire piezoelectric bilayer structure for high-temperature SAW applications,'' *IEEE Trans. Ultrason., Ferroelectr., Freq. Control*, vol. 59, no. 5, pp. 999–1005, May 2012.

[16] J. Streque, J. Camus, T. Laroche, S. Hage-Ali, H. M'Jahed, M. Rammal, T. Aubert, M. A. Djouadi, S. Ballandras, and O. Elmazria, ''Design and characterization of high-*Q* SAW resonators based on the AlN/Sapphire structure intended for high-temperature wireless sensor applications,'' *IEEE Sensors J.*, vol. 20, no. 13, pp. 6985–6991, Jul. 2020.

[17] V. S. Chivukula, D. Ciplys, R. Rimeika, M. S. Shur, J. Yang, and R. Gaska, ''Impact of photocapacitance on phase response of GaN/sapphire SAW UV sensor,'' *IEEE Sensors J.*, vol. 10, no. 4, pp. 883–887, Apr. 2010.

[18] Y. Fan, K. Xu, Z. Liu, G. Xu, H. Zhong, Z. Huang, Y. Zhang, and J. Wang, ''Ultraviolet photoresponse of surface acoustic wave device based on Fe-doped high-resistivity GaN,'' *Jpn. J. Appl. Phys.*, vol. 56, no. 5, Apr. 2017, Art. no. 050307.

[19] F. Bartoli, T. Aubert, M. Moutaouekkil, J. Streque, P. Pigeat, S. Zhgoon, A. Talbi, S. Hage-Ali, H. M'Jahed, and O. Elmazria, ''AlN/GaN/sapphire heterostructure for high-temperature packageless acoustic wave devices,'' *Sens. Actuators A, Phys.*, vol. 283, pp. 9–16, Nov. 2018.

[20] J. C. A. Ondo, E. J. J. Blampain, G. N. Mbourou, S. M. Murtry, S. Hage-Ali, and O. Elmazria, ''FEM modeling of the temperature influence on the performance of SAW sensors operating at GigaHertz frequency range and at high temperature up to 500 °C,'' *Sensors*, vol. 20, no. 15, p. 4166, Jul. 2020.

[21] W. Z. Wang, Y. Ruan, and Z. You, ''AlN/6H-SiC SAW resonator for high temperature wireless SAW sensor,'' in *Proc. 19th Int. Conf. Solid-State Sens., Actuators Microsyst. (TRANSDUCERS)*, Kaohsiung, Taiwan, Jun. 2017, pp. 942–945.

[22] V. Plessky and J. Koskela, ''Coupling-of-modes analysis of SAW devices,'' *Int. J. High Speed Electron. Syst.*, vol. 10, no. 4, pp. 867–947, Dec. 2000.

[23] K. Hashimoto, *Surface Acoustic Wave Devices in Telecommunications*, vol. 116. Berlin, Germany: Springer-Verlag, 2000.

[24] H. Chambon, P. Nicolay, G. Bruckner, and A. Benjeddou, ''Analysis of the sensitivity to pressure and temperature of a membrane based SAW sensor,'' *Int. J. Smart Nano Mater.*, vol. 8, nos. 2–3, pp. 95–109, Jul. 2017.

[25] H. Xu, H. Jin, S. Dong, X. Song, J. Chen, W. Xuan, S. Huang, L. Shi, and J. Luo, ''Mode analysis of Pt/LGS surface acoustic wave devices,'' *Sensors*, vol. 20, no. 24, p. 7111, Dec. 2020.

[26] R. R. Reeber and K. Wang, ''High temperature elastic constant prediction of some group III-nitrides,'' *MRS Internet J. Nitride Semicond. Res.*, vol. 6, no. 3, pp. 1–5, 2001.

[27] Z. D. Schwartz, A. Downey, S. Alterovitz, and G. Ponchak, ''High-temperature RF probe station for device characterization through 500 °C and 50 GHz,'' *IEEE Trans. Instrum. Meas.*, vol. 54, no. 1, pp. 369–376, Feb. 2005.

[28] G. E. Ponchak, J. L. Jordan, and M. C. Scardelletti, ''High temperature characteristics of coplanar waveguide on R-plane sapphire and alumina,'' *IEEE Trans. Adv. Packag.*, vol. 32, no. 1, pp. 146–151, Feb. 2009.

[29] S. A. Zhgoon, A. S. Shvetsov, S. A. Sakharov, and O. Elmazria, ''High-temperature SAW resonator sensors: Electrode design specifics,'' *IEEE Trans. Ultrason., Ferroelectr., Freq. Control*, vol. 65, no. 4, pp. 657–664, Apr. 2018.

[30] T. Yokoyama, T. Nishihara, S. Taniguchi, M. Iwaki, Y. Satoh, M. Ueda, and T. Miyashita, ''New electrode material for low-loss and high-*Q* FBAR filters,'' in *Proc. IEEE Ultrason. Symp.*, vol. 1, Montreal, QC, Canada, Aug. 2004, pp. 429–432.

[31] R. C. Ruby, P. Bradley, Y. Oshmyansky, A. Chien, and J. D. Larson, ''Thin film bulk wave acoustic resonators (FBAR) for wireless applications,'' in *Proc. IEEE Ultrason. Symp.*, vol. 1, Atlanta, GA, USA, Oct. 2001, pp. 813–821.

GEORGE BOLDEIU received the degree in electrical engineering from the Politehnica University of Bucharest, in 2001, and the degree in physics from the University of Bucharest, in 2014. He is currently pursuing the Ph.D. degree in the frame with the Faculty of Electronics, Telecommunications and Information Technology, Politehnica University of Bucharest. In 2001, he was hired with IMT Bucharest. Between 2007 and 2017, he worked with the Simulation Laboratory as a Simulation Engineer, being involved in the simulation of the electrical, mechanical, and thermal phenomena of MEMS devices. For a short period, from 2017 to 2019, he worked as a Thermal Simulation Engineer at Continental, Timisoara. Here, he developed and ensured thermal management for High Flash Lidar. In 2019, he returned to IMT and currently he activates in the Micromachined structures, Microwave Circuits and Devices Laboratory (RF-MEMS).

GEORGE E. PONCHAK (Fellow, IEEE) received the B.E.E. degree from Cleveland State University, OH, USA, in 1983, the M.S.E.E. degree from Case Western Reserve University, OH, USA, in 1987, and the Ph.D. degree in electrical engineering from the University of Michigan, Ann Arbor, MI, USA, in 1997. He joined the Communications, Instrumentation, and Controls Division, NASA Glenn Research Center, Cleveland, OH, USA, in 1983, and worked there through 2021 as a Senior Research Engineer. He is currently retired. In 1997 and 1998 and in 2000 and 2001, he was a Visiting Professor at Case Western Reserve University. He authored and coauthored over 200 papers in refereed journals and symposia proceedings. He was the Editor-in-Chief of IEEE Transactions Microwave Theory and Techniques (2010–2013) and IEEE Microwave and Wireless Components Letters (2006–2009). He has been served on the Editorial Board for the *International Journal of RF and Microwave Computer Aided Engineering* (2005–2019), and MDPI *Sensors* journal, since 2018. He received the 2014 N. Walter Cox Award that recognizes an IEEE MTT-S member who has given exemplary service to the Society and the Best Paper Award of the 30th International Symposium on Microelectronics.

ALEXANDRA NICOLOIU received the degree from the Faculty of Electrical Engineering, Politehnica University of Bucharest, in 2006, and the Ph.D. degree, in 2010. She has participated as a Team Member in several national and european projects, such has FP6, FP7, ESA, and ENIAC. She joined IMT-Bucharest, in 2009, in the frame of the FP7 REGPOT MIMOMEMS. Her current research interests include the numerical analysis and experimental development of GHz acoustic devices on WBG materials (GaN, AlN) working as sensors. She is involved in the team of two H2020 FET-OPEN projects dedicated to spin waves for quantum computing (''Chiron'' and ''IQubits'') and she coordinates a national project dedicated to dual temperature and pressure SAW sensors on GaN thin membranes. She is the coauthor of more than 40 papers in journals and conference proceedings. She was awarded with the Gheorghe Cartianu Prize of the Romanian Academy, in 2016.

CLAUDIA NASTASE received the Ph.D. degree from the Faculty of Physics, University of Bucharest, in 2007. She worked with the Faculty of Physics, University of Bucharest, until December 2016, where she was involved in research activities in more than 30 projects related to material physics. She is the coauthor of more than 25 papers in journals and conference proceedings. Between June 2011 and June 2012, she worked as an Associate Researcher with CEA-IRAMIS Saclay, France. Since January 2017, she has been an Employee with IMT Bucharest, where her research activities include measurements of surface acoustic wave sensing structures. She is involved in the team of two H2020 FET-OPEN projects dedicated to spin waves for quantum computing: ''Chiron'' with role in the development of magnetic sensors based on SAW devices on GaN/Si working at frequencies around ten GHz, and ''IQubits'' with role in cryogenic temperature characterization of the single electron transistor/quantum dots and qubit structures.

IOANA ZDRU received the M.Sc. degree, in 2013, and the Ph.D. degree from the Faculty of Electronics and Telecommunications, Politehnica University of Bucharest, in 2017. The subject of the Ph.D. thesis was devoted to sensors based on acoustic wave devices. She has been an Employee with IMT Bucharest stating, since April 2012. She is involved in microwave characterization of SAW devices and sensors on WBG materials. She has participated in several national and European research projects (FP7, ENIAC). She has coauthored more than 15 papers in journals and conference proceedings. She was awarded with the Gheorghe Cartianu prize of the Romanian Academy for the team work dedicated to GaN/Si SAW-based temperature sensors, in 2016.

ADRIAN DINESCU received the M.Sc. and Ph.D. degrees in solid state physics from the Faculty of Physics, University of Bucharest, in 1993 and 2010, respectively. Between 1993 and 1997, he was with the National Institute for Electronic Components Research, working in the field of optoelectronics components. Since 1997, he has been with IMT-Bucharest. He is currently the Head of the Nanoscale Structuring and Characterization Laboratory. In the last five years, he has coauthored about 75 papers in ISI journals. He was a Project Coordinator in eight national projects, the coordinator of Romanian partner (IMT-Bucharest) of the CATHERINE FP7 project, of JRP Romania—Bulgaria (''Nanostructured and amorphous semiconductor films for sensors application,'' running), and of M-ERA.NET PhotoNanoP. He is involved in the micro and nanoscale characterization using FE-SEM and in structuring at the nanoscale using Electron Beam Lithography. His expertise also includes, such as micro and nano- fabrication and optoelectronic measurements. He was awarded with the Gheorghe Cartianu prize of the Romanian Academy, in 2016.

ALEXANDRU MÜLLER (Member, IEEE) received the Ph.D. degree in semiconductor physics from the University of Bucharest, in 1990, and the Habilitation degree in electronic engineering, information technologies and telecommunications from the Politehnica University of Bucharest, in 2017. He is currently the Head of the Microwave Laboratory, IMT-Bucharest, Romania. In the recent years, his research activity was focused on SAW devices developed on III Nitrides, analysis of SAW propagation modes in GaN/Si layers, temperature and pressure sensors based on GaN/Si SAW devices, coupling of SAW waves with spin waves, cryogenic temperature measurements, in high magnetic field, of single electron transistors. He is the author/coauthor of more than 150 papers in high ranked journals and conferences proceedings. In 2003, he was invited ''Directeur de recherché'' at LAAS CNRS Toulouse, France. He was involved in many European projects (in the frame of the research EU programs FP4, FP6, FP7 and H2020) as the Coordinator or as the Leader of the IMT Team. He has coordinated one of the first European projects in RF MEMS ''MEMSWAVE'' (1998–2001), nominated in 2002 between the ten finalists for the Descartes Prize of the European Commission. He is currently involved, as the Leader of the IMT Team, in two EU founded H2020 Future Emerging Technologies (FET) call projects, connected to spin wave computing, ''Chiron'' and ''IQubits.''